STM JOURNALS

Journal of
Structural Engineering and Management

ISSN: 2393-8773
Volume 11, Issue 2, 2024
May–August
DOI (Journal): 10.37591/JoSEM

https://journals.stmjournals.com/josem/

Research JoSEM

Hygrothermal Analysis of Functionally Graded Material Plates

Huzaifa Maaz Fazlurrahman[1,*], Atteshamsuddin Sayyed[2]

Abstract

This study introduces a novel higher-order shear deformation theory, tailored to accommodate various loading conditions experienced by laminated plates. The theory is specifically designed for the hygrothermal analysis of functionally graded plates. Three homogenization methods are used to calculate the Young's modulus, namely, power law distribution, exponential distribution, and the Mori-Tanaka scheme. Navier's solution scheme is used for flexural analysis of functionally graded plates simply supported at all four edges. The results obtained for stresses and displacement are discussed and compared with previously published theories and results.

Keywords: Functionally graded plate, stress-strain relationship, displacement field, shear deformation theory, functionally graded material

INTRODUCTION

Structures that are functionally graded accomplish a specific function by continually varying the volume fractions of two or more materials based on their position along specific dimensions. Thermal barrier plate structures for high temperatures, for instance, combinations of metal and ceramic materials may find use. If necessary, the volume fractions of the two materials can be changed to shift the surface's composition from one that is rich in metal to one that is rich in ceramic. Because it has a low thermal conductivity, the material's ceramic component resists heat well. The gradual alteration of a material's characteristics can be customized for various uses and operational settings. Because of this, materials with functional gradients are preferred in many applications.

The continuous microstructure variations of functionally graded materials (FGMs) set them apart from fiber-reinforced laminated composite materials. In FGMs, the two distinct materials are bonded together, resulting in a mismatch of mechanical characteristics across an interface. Because of this, with very high thermal loading, the components of the fiber-matrix composites are prone to debonding. Furthermore, it is possible that cracks will start at the interfaces and spread to areas of the material that are weaker. The existence of residual strains brought on by the different thermal expansion coefficients of the matrix and fiber in composite materials is another issue. By gradually altering the volume proportion of the parts rather than abruptly changing them across an interface, these issues are lessened or alleviated in FGMs. FGMs have primarily been used in high-temperature situations, such as thermal shock. When the body is heated or cooled during extended periods of time, a condition is formed.

***Author for Correspondence**
Huzaifa Maaz Fazlurrahman
E-mail: huzaifamaaz0@gmail.com

[1]M. Tech Student, Department of Structural Engineering, Sanjivani College of Engineering, Kopargaon Maharashtra, India
[2]Professor, Department of Structural Engineering, Sanjivani College of Engineering, Kopargaon, Maharashtra, India

Received Date: June 03, 2024
Accepted Date: July 16, 2024
Published Date: July 18, 2024

Citation: Huzaifa Maaz Fazlurrahman, Atteshamsuddin Sayyed. Hygrothermal Analysis of Functionally Graded Material Plates. Journal of Structural Engineering and Management. 2024; 11(2): 44–62p.

Reddy [1] laid the groundwork by establishing Navier's solution for rectangular plates and finite element models based on the third-order shear

deformation plate theory. These models were developed for analyzing functionally graded plates with variations in material properties through the thickness. The plates were assumed to have an isotropic, two-constituent material distribution and a modulus that follows a power-law distribution in terms of volume percentage. The formulation incorporated geometric nonlinearity of the von Karman type, temporal dependency, and thermomechanical coupling. In a separate study, Zhu and Liew [2] introduced a local kriging meshless method for analyzing the free vibration of functionally graded circular plates subjected to thermal loading. This method utilized kriging techniques to generate meshless form functions, incorporating the Kronecker delta and properties of division of unity. Additionally, the first-order shear deformation plate theory was employed to account for transverse shear strains. The material properties are thought to be temperature-dependent and to fluctuate continuously along the thickness direction of the circular plates. Using a multi-degree-of-freedom energy method, the geometrically nonlinear parametric instability of functionally graded rectangular plates at various temperature conditions was studied by Alijani and Amabili [3]. It is assumed that the border conditions are moveable and simply supported. Collocation and pseudo-arc length continuation are the methods used for numerical studies. Transit thermoplastic difficulties involving a functionally graded plate resulting from a non-uniform heat supply were studied theoretically by Ootao and Tanigawa [4]. It is expected that the rectangular plate's thermal and thermoelastic constants change exponentially with thickness. The Laplace and finite cosine transformations are used to examine the transit three-dimensional temperatures. The general study of strain and heat stresses in a thin rotating circular disk composed of functionally graded material was developed by Chandel et al. [5]. The material properties are expressed as the power function of the direct technique used to solve the Navier and heat conduction equations, with the exception of Poisson's ratio, which is considered to depend on variable *r*. Daouadji et al. [6] developed a new higher-order shear deformation model to theoretically define the Navier solutions for rectangular plates for the static response of nine functionally graded plates. Based on the elemental volume fractions, it is believed that the plate's mechanical characteristics have a simple power law distribution that constantly varies in the thickness direction. Utilizing the proposed theory enables the straightforward and accurate examination of the static bending behavior exhibited by functionally graded plates. The effects of moisture and temperature on the bending behavior of composite functionally graded material (FGM) plates sitting on elastic foundations were studied by Zenkour et al. [7]. They examined a transverse shear and normal deformation theory that employed five unknown functions as opposed to the six or more unknown functions used in earlier shear and normal deformation theories. The hygrothermal response of functionally graded plates with simply-supported edges resting on elastic foundations provides a precise solution. Daoudadji et al. [8] introduced a novel displacement-based high-order shear deformation theory to analyze the static response of such plates. Unlike previous shear deformation hypotheses, which involved five unknown functions, this theory only involves four.

The proposed hypothesis suggests that the distribution of transverse shear stresses across the thickness follows a parabolic pattern, thereby meeting the conditions of shear stress-free surfaces. It was variationally consistent and shared many similarities with traditional plate theory. Furthermore, there was no need for a shear correction factor. Based on the volume fractions of the constituents, it is assumed that the mechanical characteristics of the plate follow a simple power law distribution that varies continuously in the thickness direction. The validity of the current hypothesis was investigated by comparing some of the findings with those of the first-order, classical, and other higher-order theories. It was discovered that the static behavior of functionally graded plates may be explained by a straightforward and precise theory. Ghugal and Sayyad [9] examined the effects of transverse shear and transverse normal strains on the static flexure of thick isotropic plates using trigonometric shear deformation theory. A novel trigonometric shared information theory for isotropic and composite laminated sandwich plates was created by Mantari et al. [10]. As the theory considers the accurate distribution of transverse shear strains across the plate thickness and enforces tangential stress-free boundary conditions on the plate's surface, the need for a shear correction factor was eliminated. The governing equations and boundary conditions for the plates were derived based on the virtual work principle. We showed the exact solutions of the Navier type for static bending analysis under sinusoidal and evenly distributed stresses. By contrasting the new theory's conclusions with other findings found

in published literature, its accuracy was verified. The outcome demonstrated that the current model looks at the ready's shear deformation theories in addition to the static behavior of isotropic and composite sandwich and laminated plates.

Thai and Kim [11] introduced an innovative higher-order shear deformation theory to analyze the bending and free vibration behavior of functionally graded plates. This theory, characterized by only four unknowns, effectively describes the parabolic variation of transverse shear strains across the plate thickness. Analytical solutions for bending and free vibration analyses of simply supported plates were derived. A comparison of the obtained results was made with predictions from various plate theories, as well as three-dimensional (3D) and quasi-3D solutions. The findings indicated that while the accuracy of the proposed theory may rival that of higher-order shear deformation theories with more unknowns, it falls short compared to the precision of 3D and quasi-3D models that consider the thickness stretching effect. Two variable refined plate theories were employed by Shimpi and Patel [12] to analyze plate free vibration. There is no elastic coupling at all; by contrasting the new theory's conclusions with other findings found in published literature, its accuracy was verified. The result showed that the present model considers not only the static behavior of isotropic and composite sandwich and laminated plates but also Reddy's shear deformation theories. By utilizing the virtual work concept, the governing equations and boundary conditions for plates were determined. Sandwich plates with varied numbers of layers were taken into account. By comparing the current theory with a variety of results from literary works, the author arrived at this conclusion. The evaluation of the static behavior of multilayered sandwich and composite plates shows that the current model outperforms all previous higher-order shear deformation theories. an investigation into the bending behavior of a FGM plate under hygro-thermo-mechanical loading conditions, supported by an elastic base. Mantari JL, Oktem AS, Soares CG, they employed a four-variable refined plate theory, which adequately accounts for the quadratic variation of transverse shear stresses across the plate thickness and satisfies zero traction boundary conditions on both the top and bottom surfaces [13]. Notably, this theory features four independent unknowns, unlike previous shear deformation theories that typically involve five. It is believed that the elastic, thermal, and moisture expansion coefficients of the plate are graded in the direction of thickness. The elastic foundation is modeled using a two-parameter Pasternak foundation. The accuracy of the current theory is confirmed by numerical findings, and the effects of various parameters are examined. This topic is relevant to the modeling of rocket launch pad structures under high heat loads [13–16].

Mathematical Formulation

FGMs are quite diverse, yet it is useful to idealize them such that their mechanical properties vary smoothly with spatial coordinates. This idealization produces closed-form solutions to some fundamental problems in solid mechanics and helps with the creation of numerical models of structures made of FGMs (Figure 1). It is commonly considered that the qualities of the material gradation continuously over the thickness

Examine a plate with sides “a” and “b” and a total thickness of h. The material used in the plate is functionally graded across the thickness (Figure 1). Different loading conditions and boundaries are applied to the plate. In Cartesian coordinate system, the plate lies in the region $0 \leq x \leq a$, $0 \leq y \leq b$, $-h/2 \leq z \leq h/2$. On the plate's upper surface, a transverse load q(x, y) is applied (i.e., z = -h/2). It is anticipated that the material properties of FG plates change steadily as they get thicker. The following three homogenization techniques are used to determine Young's modulus E(z):

1. The power law distribution.
2. The exponential distribution.
3. The Mori-Tanaka scheme.

For the power law distribution, Young's modulus is given as

$$E(Z)= E_m+ (E_c – E_m) (0.5+z/h)^n \quad (1)$$

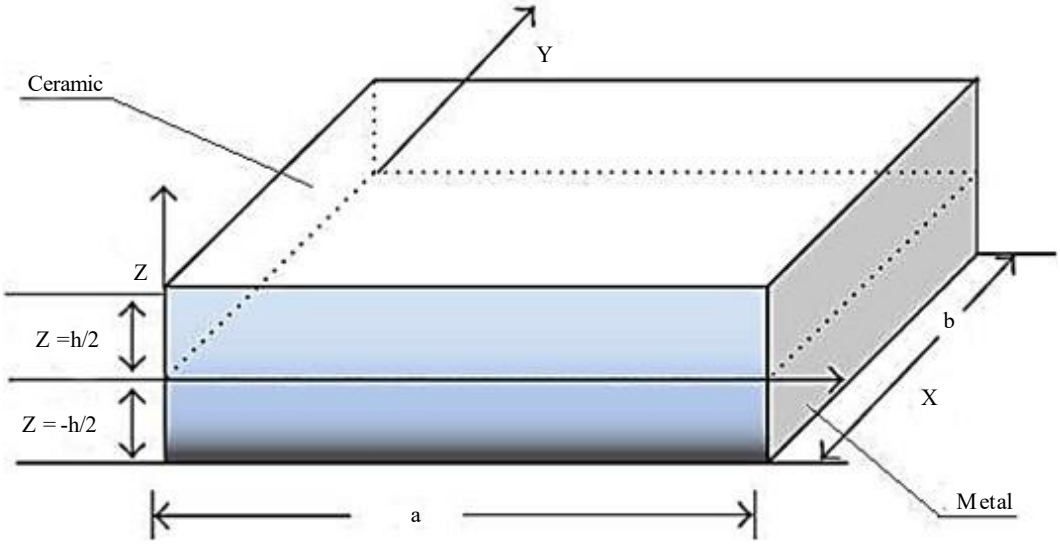

Figure 1. Geometry of rectangular plate composed of functionally graded material (FGM).

where 'n' is the power law index, and the subscript 'm' and 'c' represent the metallic and ceramic constants, respectively (Figure 2).

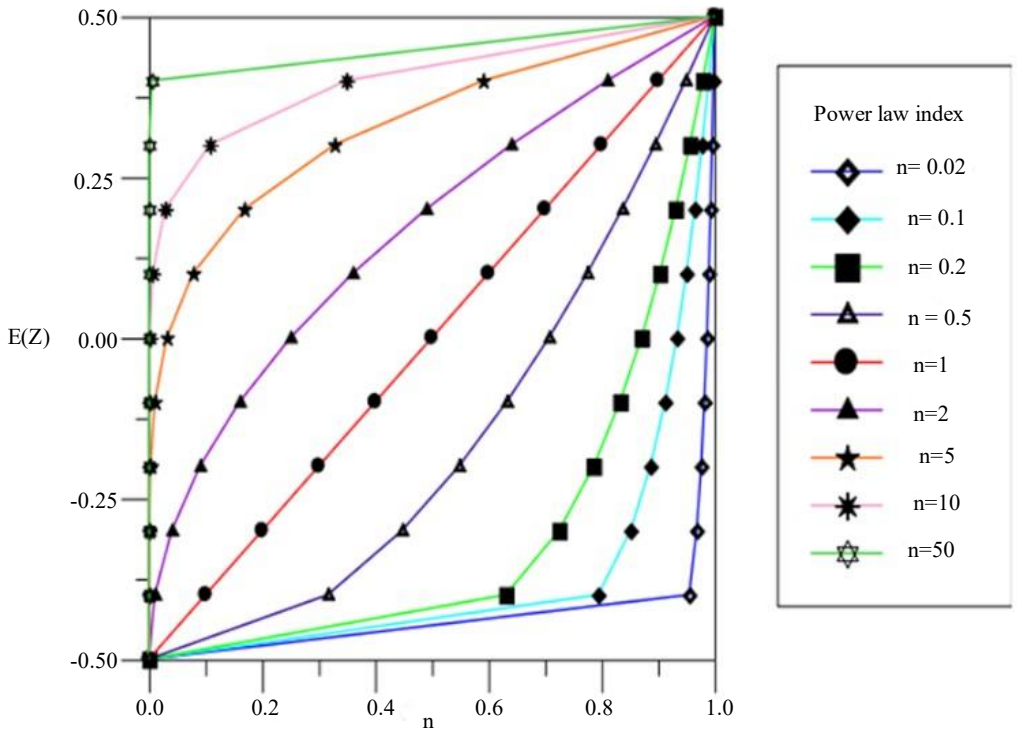

Figure 2. Variations of Young's modulus through the depth of functionally graded material (FGM) plate for various values of power law index n.

Assumptions made in the mathematical formulation

The following presumptions form the foundation of the current theory's mathematical formulation.

- Since the displacements are negligible in relation to the thickness of the plate, the strains involved are also negligible.
- There is shear, bending, and extension components to the displacements u in the x-direction and v in the y-direction.

- Shear and bending are the two components that make up the transverse displacement.
- The only load applied to the plate is transverse load.
- The powers of the body are disregarded.

Displacement Field, Strains, Stresses, and Stress Resultants

Displacement field

The following displacement field connected to the current theory is derived from the aforementioned assumptions:

$$U(x,y,z) = u\_0\text{-}z\ \ 〚\partial w〛\_b/\partial x\text{-}f(z)\ \ 〚\partial w〛\_s/\partial x$$
$$V(x,y,z) = v\_0\text{-}z\ \ 〚\partial w〛\_b/\partial y\text{-}f(z)\ \ 〚\partial w〛\_s/\partial y \quad (2)$$
$$W(x,y,z) = w\_b\ (x,y)+w\_s\ (x,y)$$

Strain-Displacement Relationships

Within the framework of the linear theory of elasticity, normal strains (ε_x and ε_y) and shear strains (η_{zx}, η_{zy}, γ_{xy}) are determined using the displacement field provided by Equation (2)

$$\varepsilon_{xx} = \left[\frac{\partial u_0}{\partial x} - z\frac{\partial^2 w_b}{\partial x^2} - f(z)\frac{\partial^2 w_s}{\partial x^2}\right]$$
$$\varepsilon_{yy} = \left[\frac{\partial v_0}{\partial y} - z\frac{\partial^2 w_b}{\partial y^2} - f(z)\frac{\partial^2 w_s}{\partial y^2}\right] \quad (3)$$
$$\gamma_{zx} = \left[1 - \frac{\partial f(z)}{\partial z}\right]\frac{\partial w_s}{\partial x}\ ,\ \gamma_{yz} = \left[1 - \frac{\partial f(z)}{\partial z}\right]\frac{\partial w_s}{\partial y}$$
$$\gamma_{xy} = \left[\frac{\partial u_0}{\partial y} + \frac{\partial v_0}{\partial x} - 2z\frac{\partial^2 w_b}{\partial x \partial y} - 2f(z)\frac{\partial^2 w_s}{\partial x \partial y}\right]$$

Stress-Strain Relationships

Transverse normal stress σ_z has a negligible effect on the gross response of an isotropic material plate with constant thickness compared to the following constitutive relations: in-plan stresses σ_x and σ_y are related to normal strains (ε_x and ε_y); shear stresses τ_{xy}, τ_{yz}, and τ_{xz} are related to shear strains γ_{xy}, γ_{yz}, and γ_{xz}.

$$\begin{Bmatrix} \sigma_{xx} \\ \sigma_{yy} \\ \tau_{yz} \\ \tau_{xz} \\ \tau_{xy} \end{Bmatrix} = \begin{bmatrix} Q_{11} & Q_{12} & 0 & 0 & 0 \\ Q_{12} & Q_{22} & 0 & 0 & 0 \\ 0 & 0 & Q_{33} & 0 & 0 \\ 0 & 0 & 0 & Q_{44} & 0 \\ 0 & 0 & 0 & 0 & Q_{55} \end{bmatrix} \left[\begin{Bmatrix} \varepsilon_{xx} \\ \varepsilon_{yy} \\ \gamma_{yz} \\ \gamma_{xz} \\ \gamma_{xy} \end{Bmatrix} - \begin{Bmatrix} \alpha_t + \beta_c \\ \alpha_t + \beta_c \\ 0 \\ 0 \\ 0 \end{Bmatrix} \right] \quad (4)$$

Governing Equations and Boundary Conditions

The notion of virtual work can be utilized to generate the boundary conditions and variationally consistent governing equation of equilibrium related to the current theory. The principle of virtual work can be expressed analytically as

$$\int_0^a \int_0^b q\delta w dx\, dy = \int_0^a \int_0^b \int_{-h/2}^{+h/2} \begin{pmatrix} \sigma_x \delta\varepsilon_x + \sigma_y \delta\varepsilon_y + \tau_{xy}\delta\gamma_{xy} + \tau_{xz}\delta\varepsilon_{xz} \\ + \tau_{yz}\delta\gamma_{yz} \end{pmatrix} dx dy dz \quad (5)$$

The arbitrary variations may appear here. By dissecting the above equation into its constituent parts and collecting the coefficients of each, one can derive the governing equation of equilibrium and boundary conditions associated with the present theory.

The governing equations of equilibrium are as follows:

$$\delta u_0 : \frac{\partial N_x}{\partial x} + \frac{\partial N_{xy}}{\partial y} = 0 \quad (6)$$

$$\delta v_0 : \frac{\partial N_y}{\partial y} + \frac{\partial N_{xy}}{\partial x} = 0 \quad (7)$$

$$\delta w_b : \frac{\partial^2 M_x^b}{\partial x^2} + \frac{\partial^2 M_y^b}{\partial y^2} + 2\left[\frac{\partial^2 M_{xy}^b}{\partial x \partial y}\right] = q \quad (8)$$

$$\delta w_s : \frac{\partial^2 M_x^s}{\partial x^2} + \frac{\partial^2 M_y^s}{\partial y^2} + 2\left[\frac{\partial^2 M_{xy}^s}{\partial x \partial y}\right] - \frac{\partial s_x}{\partial x} - \frac{\partial s_y}{\partial y} = q \quad (9)$$

Where Axial force resultants are

$$N_x = A_{11}\left[\frac{\partial u_0}{\partial x} - \alpha T_1 - \beta C_1\right] + B_{11}\left[\frac{\partial^2 w_b}{\partial x^2} - \frac{\alpha}{h}T_2 - \frac{\beta}{h}C_2\right] + C_{11}\left[\frac{-\partial^2 w_s}{\partial x^2} - \frac{\alpha}{h}T_3 - \frac{\beta}{h}C_3\right] + A_{12}\left[\frac{\partial v_0}{\partial y} - \alpha T_1 - \beta C_1\right] + B_{12}\left[\frac{-\partial^2 w_b}{\partial y^2} - \frac{\alpha}{h}T_2 - \frac{\beta}{h}C_2\right] + C_{12}\left[\frac{-\partial^2 w_s}{\partial y^2} - \frac{\alpha}{h}T_3 - \frac{\beta}{h}C_3\right] \quad (10)$$

$$N_y = A_{12}\frac{\partial u_0}{\partial x} - B_{12}\frac{\partial^2 wb}{\partial x^2} - C_{12}\frac{\partial^2 ws}{\partial x^2} - T_1 A_{T12} - \frac{1}{h}T_2 B_{T12} - \frac{1}{h}T_3 C_{T12} - C_1 A_{C12} - \frac{1}{h}C_2 B_{C12} - \frac{1}{h}C_3 C_{C12} + A_{22}\frac{\partial v_0}{\partial y} - B_{22}\frac{\partial^2 w_b}{\partial y^2} - C_{22}\frac{\partial^2 w_s}{\partial y^2} - T_1 A_{T22} - \frac{1}{h}T_2 B_{T22} - \frac{1}{h}T_3 C_{T22} - C_1 A_{C22} - \frac{1}{h}C_2 B_{C22} - \frac{1}{h}C_3 C_{C22} \quad (11)$$

$$N_{xy} = A_{55}\frac{\partial u_0}{\partial y} + A_{55}\frac{\partial v_0}{\partial x} - 2B_{55}\frac{\partial^2 w_b}{\partial x \partial y} - 2C_{55}\frac{\partial^2 w_s}{\partial x \partial y} \quad (12)$$

$$M_x^b = B_{11}\frac{\partial u_0}{\partial x} - D_{11}\frac{\partial^2 wb}{\partial x^2} - F_{11}\frac{\partial^2 w_s}{\partial x^2} - T_1 B_{T11} - \frac{1}{h}T_2 D_{T11} - \frac{1}{h}T_3 F_{T11} - C_1 B_{11} - \frac{1}{h}C_2 D_{11} - \frac{1}{h}C_3 F_{11} + B_{12}\frac{\partial v_0}{\partial y} - D_{12}\frac{\partial^2 w_b}{\partial y^2} - F_{12}\frac{\partial^2 w_s}{\partial y^2} - T_1 B_{T12} - \frac{1}{h}T_2 D_{T12} - \frac{1}{h}T_3 F_{T12} - C_1 B_{12} - \frac{1}{h}C_2 D_{12} - \frac{1}{h}C_3 F_{12} \quad (13)$$

$$M_{xy}^b = B_{55}\frac{\partial u_0}{\partial y} + B_{55}\frac{\partial v_0}{\partial x} - 2D_{55}\frac{\partial^2 w_b}{\partial x \partial y} - 2F_{55}\frac{\partial^2 w_s}{\partial x \partial y} \quad (14)$$

$$M_{xy}^s = C_{55}\frac{\partial u_0}{\partial y} + C_{55}\frac{\partial v_0}{\partial x} - 2F_{55}\frac{\partial^2 w_b}{\partial x \partial y} - 2H_{55} \quad (15)$$

$$S_x = J_{44}\frac{\partial w_s}{\partial_x} \ , \ S_y = J_{33}\frac{\partial w_s}{\partial_x} \quad (16)$$

$$M_y^s = C_{12}\frac{\partial u_0}{\partial x} - F_{12}\frac{\partial^2 wb}{\partial x^2} - H_{12}\frac{\partial^2 w_s}{\partial x^2} - T_1 C_{T12} - \frac{1}{h}T_2 F_{T12} - \frac{1}{h}T_3 H_{T12} - C_1 C_{C12} - \frac{1}{h}C_2 F_{C12} - \frac{1}{h}C_3 H_{C12} + C_{22}\frac{\partial v_0}{\partial y} - F_{22}\frac{\partial^2 w_b}{\partial y^2} - H_{22}\frac{\partial^2 w_s}{\partial y^2} - T_1 C_{T11} - \frac{1}{h}T_2 F_{T22} - \frac{1}{h}T_3 F_{T22} - C_1 C_{C22} - \frac{1}{h}C_2 F_{C22} - \frac{1}{h}C_3 H_{C22} \quad (17)$$

By substituting these above values in eq. (3.6), (3.7), (3.8) & (3.9) We get force vectors are as follows:

$$F_1 = \alpha T_{1mn} + \frac{1}{h}\alpha T_{2mn}[BT_{11} + BT_{12}] + \frac{1}{h}\alpha T_{3mn}[CT_{11} + CT_{12}] + \alpha C_{1mn}[AC_{11} + AC_{12}] + \frac{1}{h}\alpha C_{2mn}[BC_{11} + BC_{12}] + \frac{1}{h}\alpha C_{3mn}[CC_{11} + CC_{12}]$$

$$F_2 = \beta T_{1mn}[AT_{12} + AT_{22}] + \frac{1}{h}\beta T_{2mn}[BT_{12} + BT_{22}] + \frac{1}{h}\beta T_{3mn}[CT_{12} + CT_{22}] + \beta C_{1mn}[AC_{12} + AC_{22}] + \frac{1}{h}\beta C_{2mn}[BC_{12} + BC_{22}] + \frac{1}{h}\beta C_{3mn}[CC_{12} + CC_{22}]$$

$$F_3 = q_{mn} + \alpha^2 T_{1mn}[BT_{11} + BT_{12}] + \frac{1}{h}\alpha^2 T_{2mn}[DT_{11} + DT_{12}] + \frac{1}{h}\alpha^2 T_{3mn}[FT_{11} + FT_{12}] + \alpha^2 C_{1mn}[BC_{11} + BC_{12}] + \frac{1}{h}\alpha^2 C_{2mn}[DC_{11} + DC_{12}] + \frac{1}{h}\alpha^2 C_{3mn}[FC_{11} + FC_{12}] + \beta^2 T_{1mn}[BT_{12} + BT_{22}] + \frac{1}{h}\beta^2 T_{2mn}[DT_{12} + DT_{22}] + \frac{1}{h}\beta^2 T_{3mn}[FT_{12} + FT_{22}] + \beta^2 C_{1mn}[BC_{12} + BC_{22}] + \frac{1}{h}\beta^2 C_{2mn}[DC_{12} + DC_{22}] + \frac{1}{h}\beta^2 C_{3mn}[FC_{12} + FC_{22}]$$

Navier Solution for Simply Supported Plates

The flexural analysis of functionally graded plates simply supported at all four edges is performed using the Navier solution scheme that follows. The transverse load q(x,y) is applied to the plate at its

top surface, or = -h/2. The sinusoidally distributed load in double trigonometric series is presented in the equation.

$$q(x,y) = \sum_{m=1,3,5}^{\infty} \sum_{n=1,3,5}^{\infty} q_{mn} \sin \alpha x \sin \beta y \tag{18}$$

The following solution form is assumed for unknown displacement variable δu_0, δv_0, δw_b, δw_s, satisfying the boundary conditions for simply supported plates exactly.

$$\begin{Bmatrix} u_0 \\ v_0 \\ w_b \\ w_s \end{Bmatrix} = \begin{Bmatrix} u_{mn} \cos \alpha x \sin \beta y \\ v_{mn} \sin \alpha x \cos \beta y \\ w_{bmn} \sin \alpha x \sin \beta y \\ w_{smn} \sin \alpha x \sin \beta y \end{Bmatrix} \tag{19}$$

where $u_{mn}, v_{mn}, w_{bmn}, and\ w_{smn}$ are arbitrary constants, $\alpha = m\pi/a \ and \quad \beta = n\pi/b$ also q_0 is the maximum intensity of load at the center of the load. The following matrix form is obtained by substituting this solution form and the transverse load q(x,y) into the governing equations.

$$\begin{bmatrix} k_{11} & k_{12} & k_{13} & k_{14} \\ k_{21} & k_{22} & k_{23} & k_{24} \\ k_{31} & k_{32} & k_{33} & k_{34} \\ k_{41} & k_{42} & k_{43} & k_{44} \end{bmatrix} \begin{Bmatrix} u_{mn} \\ v_{mn} \\ w_{bmn} \\ w_{smn} \end{Bmatrix} \begin{Bmatrix} 0 \\ 0 \\ q_{mn} \\ q_{mn} \end{Bmatrix} \tag{20}$$

where stiffness matrix $[K]$ is as follows:

$$K_{11} = -[A_{11}\alpha^2 + A_{55}\beta^2]$$
$$K_{12} = -[A_{12} + A_{55}]\alpha\beta$$
$$K_{13} = [B_{11}\alpha^3 + (B_{12} + 2B_{55})\alpha\beta^2]$$
$$K_{14} = [C_{11}\alpha^3 + (C_{12} + 2C_{55})\alpha\beta^2]$$
$$K_{21} = -[A_{12} + A_{55}]\alpha\beta$$
$$K_{22} = -[A_{22}\beta^2 + A_{55}\alpha^2]$$
$$K_{23} = [(B_{12} + 2B_{55})\alpha^2\beta + B_{22}\beta^3]$$
$$K_{24} = [C_{22}\beta^3 + (C_{12} + 2C_{55})\alpha^2\beta]$$
$$K_{31} = [B_{11}\alpha^3 + (B_{12} + 2B_{55})\alpha\beta^2]$$
$$K_{32} = [(B_{12} + 2B_{55})\alpha^2\beta + B_{22}\beta^3]$$
$$K_{33} = -[D_{11}\alpha^4 + (2D_{12} + 4D_{55})\alpha^2\beta^2 + D_{22}\beta^4]$$
$$K_{34} = -[F_{11}\alpha^4 + (2F_{12} + 4F_{55})\alpha^2\beta^2 + F_{22}\beta^4]3.21$$
$$K_{41} = [C_{11}\alpha^3 + (C_{12} + 2C_{55})\alpha\beta^2]$$
$$K_{42} = [C_{22}\beta^3 + (C_{12} + 2C_{55})\alpha^2\beta]$$
$$K_{43} = -[F_{11}\alpha^4 + (2F_{12} + 4F_{55})\alpha^2\beta^2 + F_{22}\beta^4]$$
$$K_{44} = -[H_{11}\alpha^4 + H_{22}\beta^4 + (2H_{12} + 4H_{55})\alpha^2\beta^2 + J_{44}\alpha^2 + J_{33}\beta^2]$$
$$K_{21} = K_{12}\,, K_{31} = K_{13}\,, K_{32} = K_{23}\,, K_{41} = K_{14} \quad , \ K_{43} = K_{34}$$

where

$$A_{ij} = Q_{ij} \int_{-h/2}^{+h/2} dz \quad , \quad B_{ij} = Q_{ij} \int_{-h/2}^{+h/2} z dz$$

$$C_{ij} = Q_{ij} \int_{-h/2}^{+h/2} f(z) dz \quad , \ D_{ij} = Q_{ij} \int_{-h/2}^{+h/2} z^2 dz$$

$$F_{ij} = Q_{ij} \int_{-h/2}^{+h/2} z f(z) dz \ , H_{ij} = Q_{ij} \int_{-h/2}^{+h/2} [f(z)]^2 dz$$

$$J_{ij} = Q_{ij} \int_{-h/2}^{+h/2} [g(z)]^2 dz$$

The unknown coefficients u_{mn}, v_{mn}, w_{bmn}, and w_{smn} can be found from the solution of Equation (20). After obtaining the values of these coefficients, one can use the plate to determine every component of displacement and stress.

NUMERICAL RESULTS

We will now compare and discuss the results obtained for displacements and stresses with the corresponding results of Zenkour et al.'s [7] higher-order shear deformation theory and Zidi et al.'s [16] refined plate theory. To facilitate the presentation of the study's findings, the numerical results are provided in the following non-dimensional format Table 1.

In Zenkour et al.'s paper [7], the following non-dimensional parameters are used:

$$\bar{w} = \frac{10h^3 E_C}{q_0 a} w\left(\frac{a}{2}, \frac{b}{2}, \frac{z}{h}\right) \ , \ \overline{\sigma_x} = \frac{h}{q_0 a} \sigma_x \left(\frac{a}{2}, \frac{b}{2}, \frac{z}{h}\right)$$

$$\overline{\tau_{xz}} = \frac{10h}{q_0 a} \tau_{xz} \left(0, \frac{b}{2}, \frac{z}{h}\right) \ , \ \overline{\tau_{xy}} = \frac{h}{q_0 a} \tau_{xy} \left(0,0, \frac{z}{h}\right)$$

$$\overline{\tau_{yz}} = \frac{10}{q_0} \tau_{yz} \left(\frac{a}{2}, 0, \frac{z}{h}\right)$$

In Zidi et al.'s paper [16], the following non-dimensional parameters were used.

Table 1. Material properties used in the functionally graded (FG) plate

Mechanical Hygro-Thermal				
Properties	**Aluminum**	**Alumina**	**Titanium**	**Zirconium**
E	70	380	130	130
μ	0.3	0.3	0.33	0.33
A	0	0	10.3	7.11
B	0	0	0.33	0

$$\bar{w} = \frac{10h^2 D}{a^4 q_0} w\left(\frac{a}{2}, \frac{b}{2}\right) \ , \ \overline{\sigma_x} = \frac{1}{10^2 q_0} \sigma_x \left(\frac{a}{2}, \frac{b}{2}, \frac{h}{2}\right)$$

$$\overline{\tau_{xy}} = \frac{1}{10 q_0} \tau_{xy} \left(0,0, -\frac{h}{3}\right) \ , \ \overline{\tau_{xz}} = \frac{1}{10 q_0} \tau_{xz} \left(0, \frac{b}{2}, 0\right)$$

The following material attributes are assumed to be present in the titanium and zirconium that make up the FGM plate:

Metal (titanium): $\mathrm{E_M} = 66.2$ GPa

Ceramic (zirconium): $\mathrm{E_C} = 117.00$ GPa

FGM: $E(Z) = E_M + (E_C - E_M)\left(0.5 + \frac{z}{h}\right)^n$

$G = \frac{E(z)}{2(1-\mu)}$

where μ is Poisson's ratio, *G* is the shear modulus, and *E* is the Young's modulus.

Calculate the percentage error between the theoretical conclusion and the exact elasticity solution.

RESULTS AND DISCUSSION

Tables 2 and 3 illustrate how the volume fraction exponent affects the dimensionless stresses and displacements of the FGM square plate (a/h = 10). Table 2 presents comparisons between the obtained

results for plates subjected to uniform and sinusoidally distributed loads, respectively, and the generalized normal deformation theory by Zenkour. The homogeneous distribution of loads is known to invariably overestimate the displacements and stresses. The difference diminishes for in-plane normal stresses σ_y and increases for deflections and in-plane longitudinal stress σ_x as the plate gets more and more metallic. It is significant to note that a totally metal plate and a wholly ceramic plate experience the same stresses. This is because the stresses in these two scenarios are independent of the modulus of elasticity and the plate is completely homogeneous.

Table 2. Under sinusoidal loads, the nondimensionalized deflection W1(0) and the in-plane normal stress Σ1(H/3) in functionally graded material (FGM) plates have been observed.

		W1			**σ1**		
P	***Theory***	***4***	***10***	***100***	***4***	***10***	***100***
1	Present	0.726	0.589	0.562	0.567	1.461	14.692
	Zenkour et al.	0.689	0.568	0.544	0.570	1.415	14.134
4	Present	1.165	0.883	0.828	0.424	1.141	1.569
	Zenkour et al.	1.097	0.840	0.791	0.418	1.080	10.863
10	Present	1.393	1.011	0.936	0.420	0.847	8.623
	Zenkour et al.	1.333	0.980	0.913	0.303	0.803	8.111

Table 3. Nondimensionalized deflection W1(0) of and the in-plane normal stress σ1(h/3) in functionally graded material (FGM) plates under uniformly distributed loads.

	P				
a/h	***Theory***	***1***	***2***	***5***	***10***
5	Present	1.1481	1.4894	1.9015	2.1436
	Zenkour et al.	0.99834	1.27965	1.61486	1.83985
10	Present	0.9936	1.2782	1.5486	1.7148
	Zenkour et al.	0.89608	1.13521	1.37405	1.5436
20	Present	0.9539	1.2237	1.4565	1.6028
	Zenkour et al.	0.87031	1.09882	1.31341	1.46903
50	Present	0.9427	1.2083	1.4304	1.5710
	Zenkour et al.	0.86308	1.08715	1.29640	1.44810
100	Present	0.9411	1.2061	1.4266	1.5664
	Zenkour et al.	0.86205	1.08715	1.29397	1.4454

Table 3 displays the volume fraction exponent ratio P, elastic foundation parameters, and magnitude less deflection and stresses of the FGM rectangular plate.

The dimensionless displacements and stresses of the FGM rectangular plate under mechanical load are analyzed in Table 4 and are related to the elastic foundation parameters and the volume fraction exponent ratio P. It is clear that less stresses and deflection occur when the elastic basis is present.

The deflection for FGM plates will increase as the volume fraction exponent rises. The variations in P also have an impact on the stresses.

Similar findings to those in Table 4 are shown in Table 5, which also includes the impact of the moisture and temperature fields. The outcomes that were predicted by first-order, second-order, and third-order shear deformation theories are contrasted with the actual results. The current theory and TSDT exhibit a high degree of agreement for all power law index n values, both with and without the elastic foundation. The stresses for a wholly ceramic plate differ from those of a fully metal plate with an elastic substrate, and this is a crucial observation to make. This is due to the fact that the temperature field's inclusion has an impact on this plate (Figures 3–16).

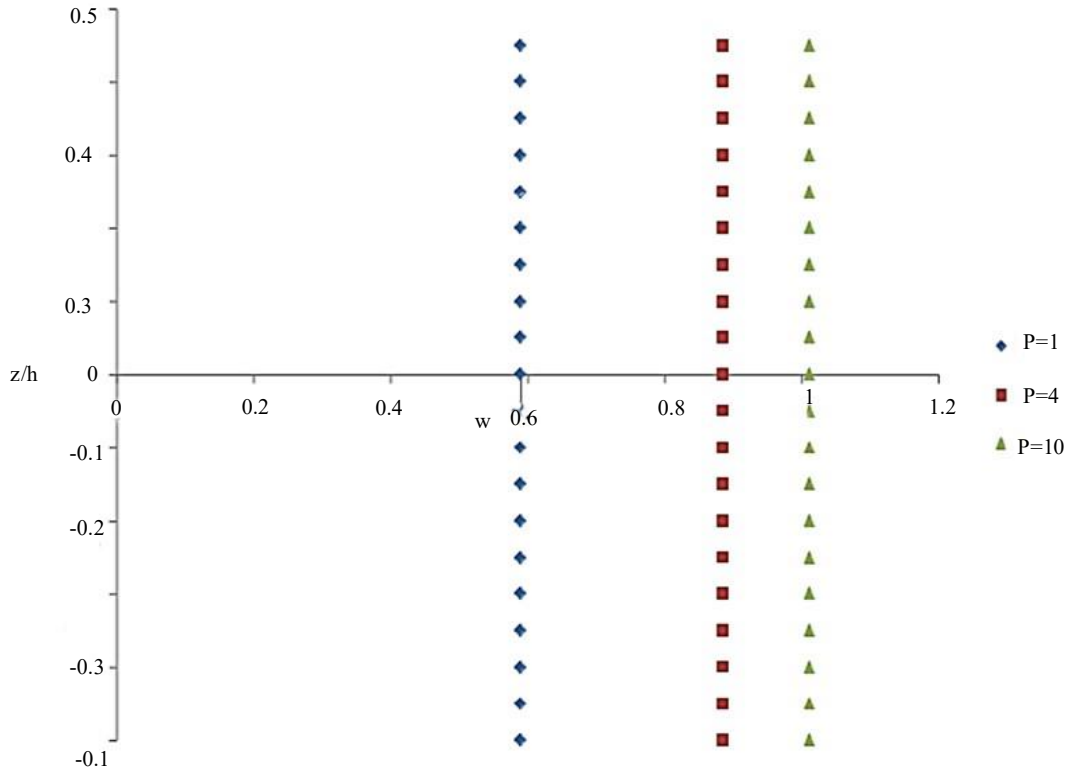

Figure 3. Nondimensionalized deflection w1 versus thickness ratio (z/h) in functionally graded (FG) plate under sinusoidal loads (a/h = 10).

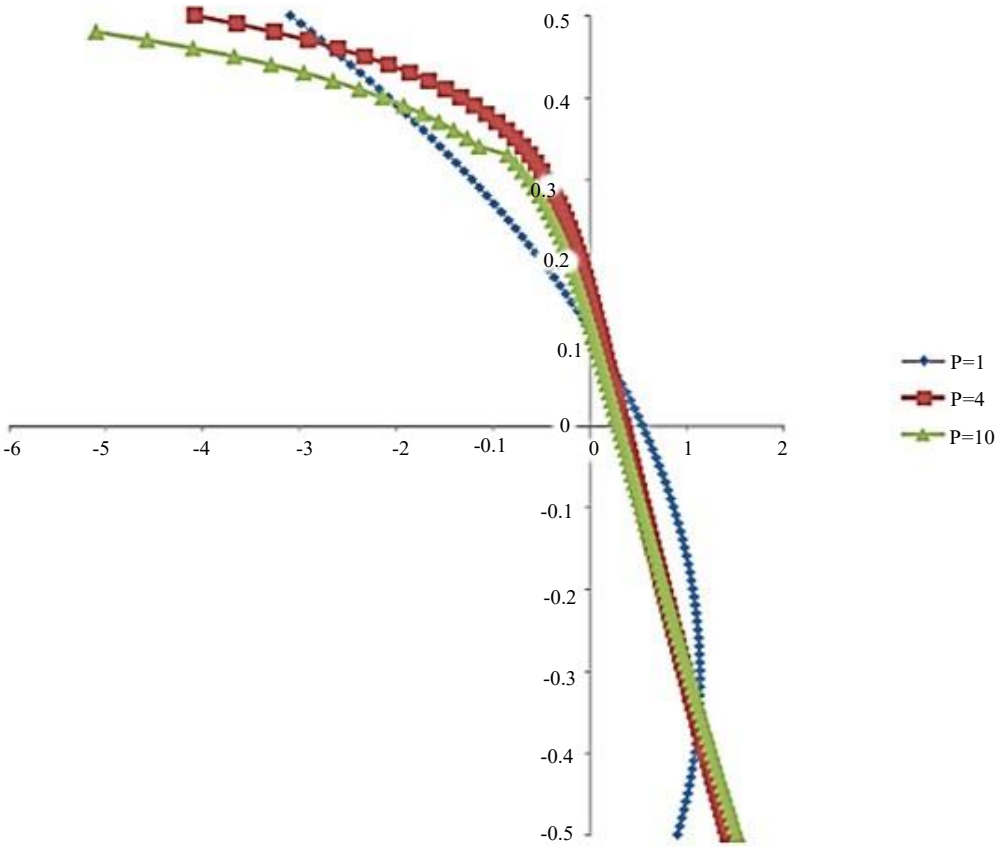

Figure 4. Nondimensionalized deflection σ1 versus thickness ratio (z/h) in functionally graded (FG) plate under sinusoidal loads (a/h = 10).

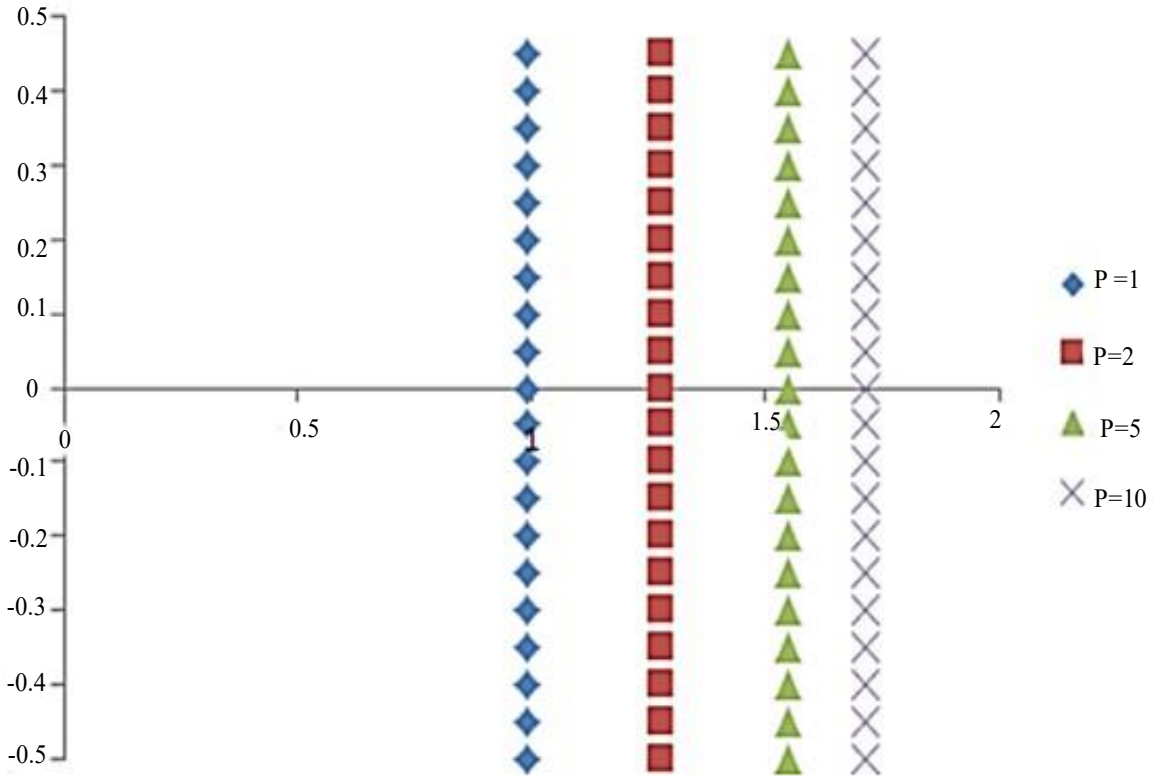

Figure 5. Nondimensionalized deflection w1 versus thickness ratio (z/h) in functionally graded (FG) plate under uniformly distributed loads (a/h = 10).

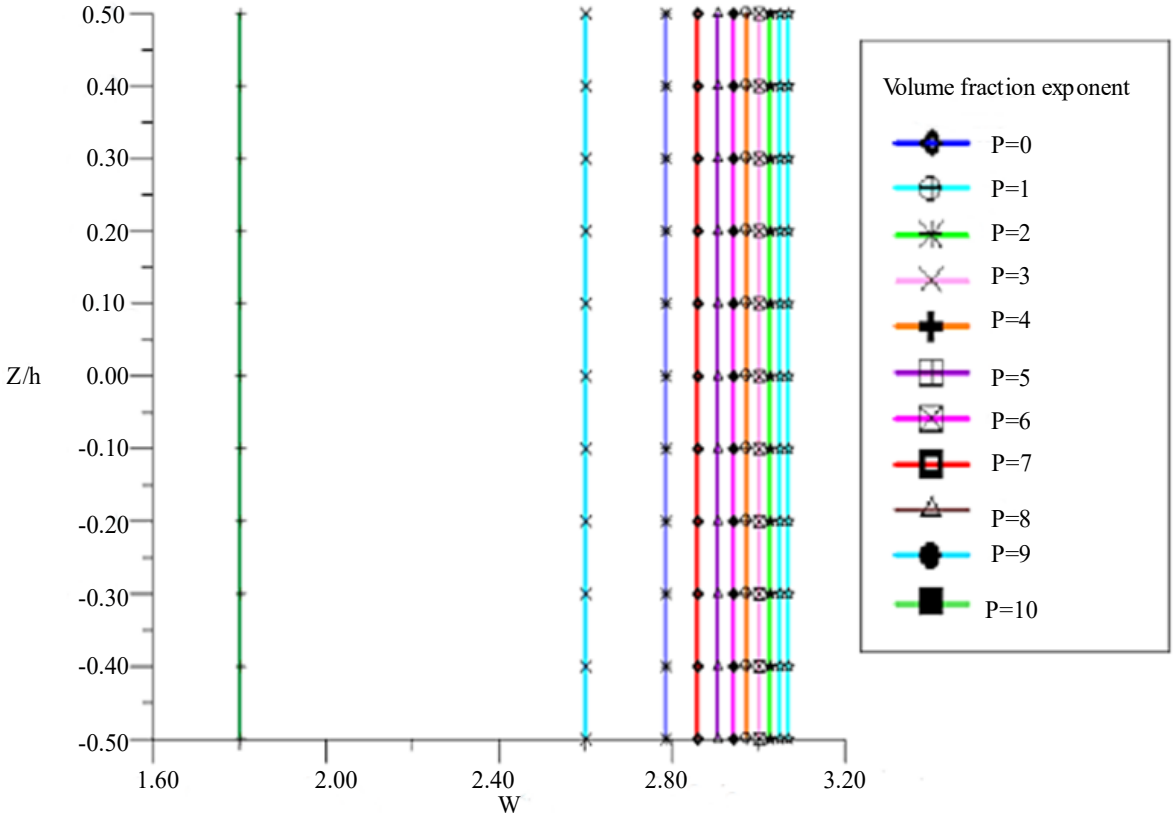

Figure 6. Dimensionless center of deviation (w) for functionally graded material (FGM) rectangular plate under mechanical loading plotted against thickness ratio (z/h).

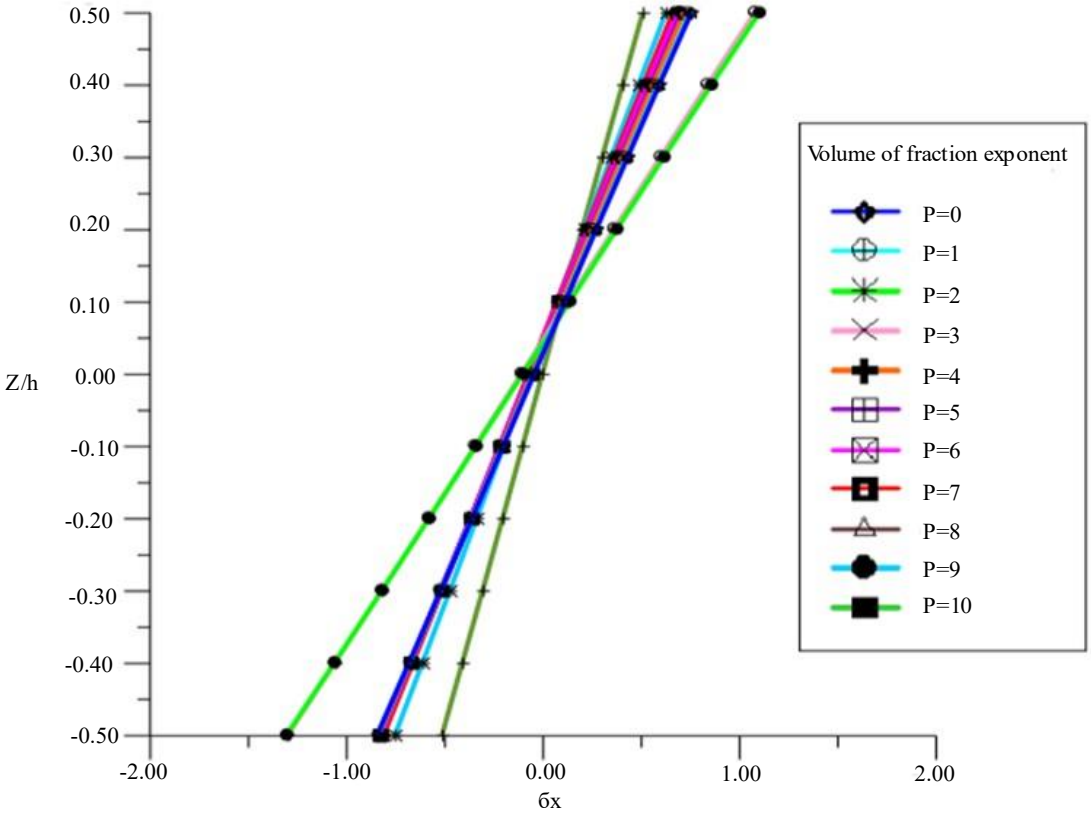

Figure 7. Dimensionless normal stress σ_x versus the thickness ratio of z/h for functionally graded material (FGM) rectangular plate under mechanical loading.

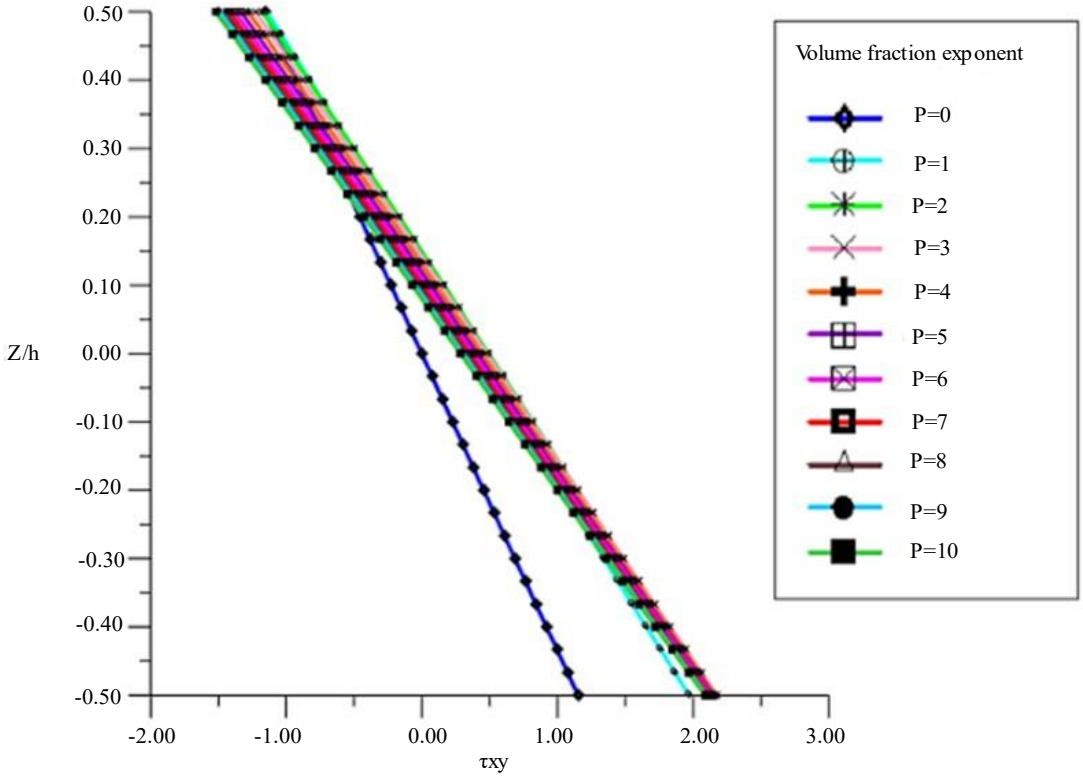

Figure 8. Dimensionless shear stress τ_{xy} versus thickness ratio of z/h for functionally graded material (FGM) rectangular plate under mechanical loading

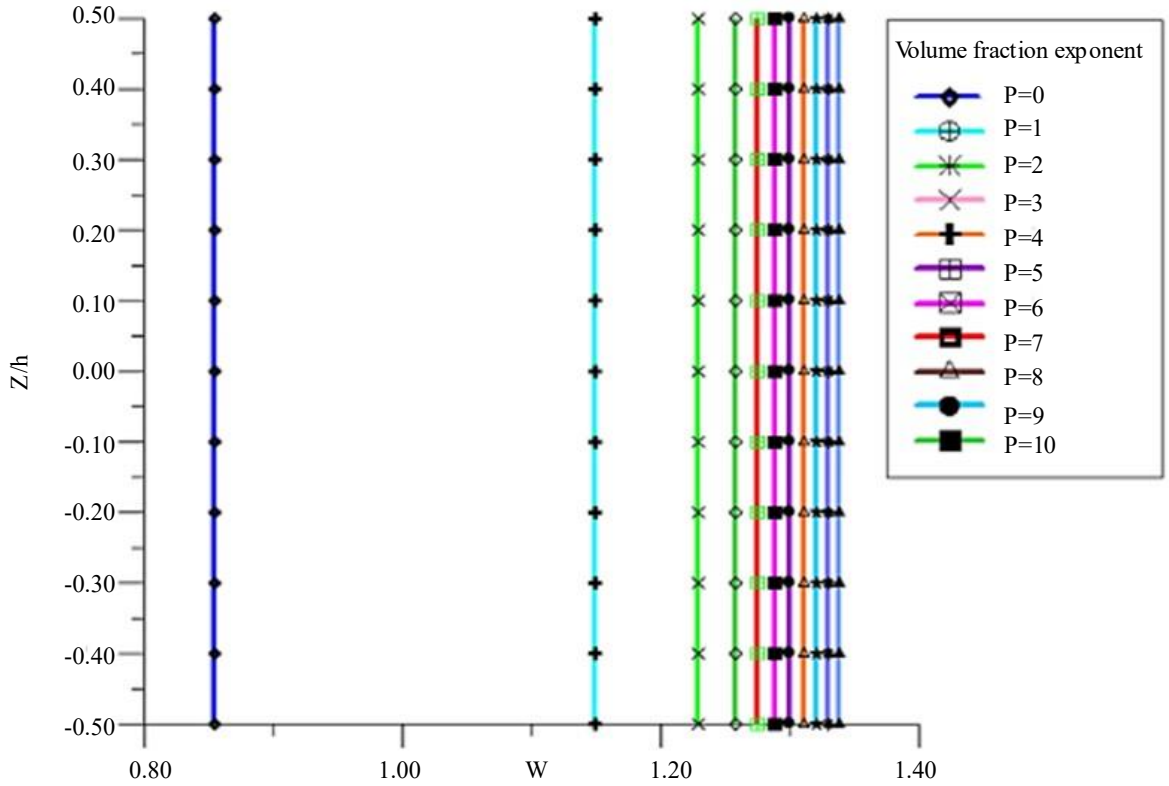

Figure 9. The functionally graded material (FGM) rectangular plate's dimensionless center deflection (w) is plotted against the thickness ratio (z/h) under linear force.

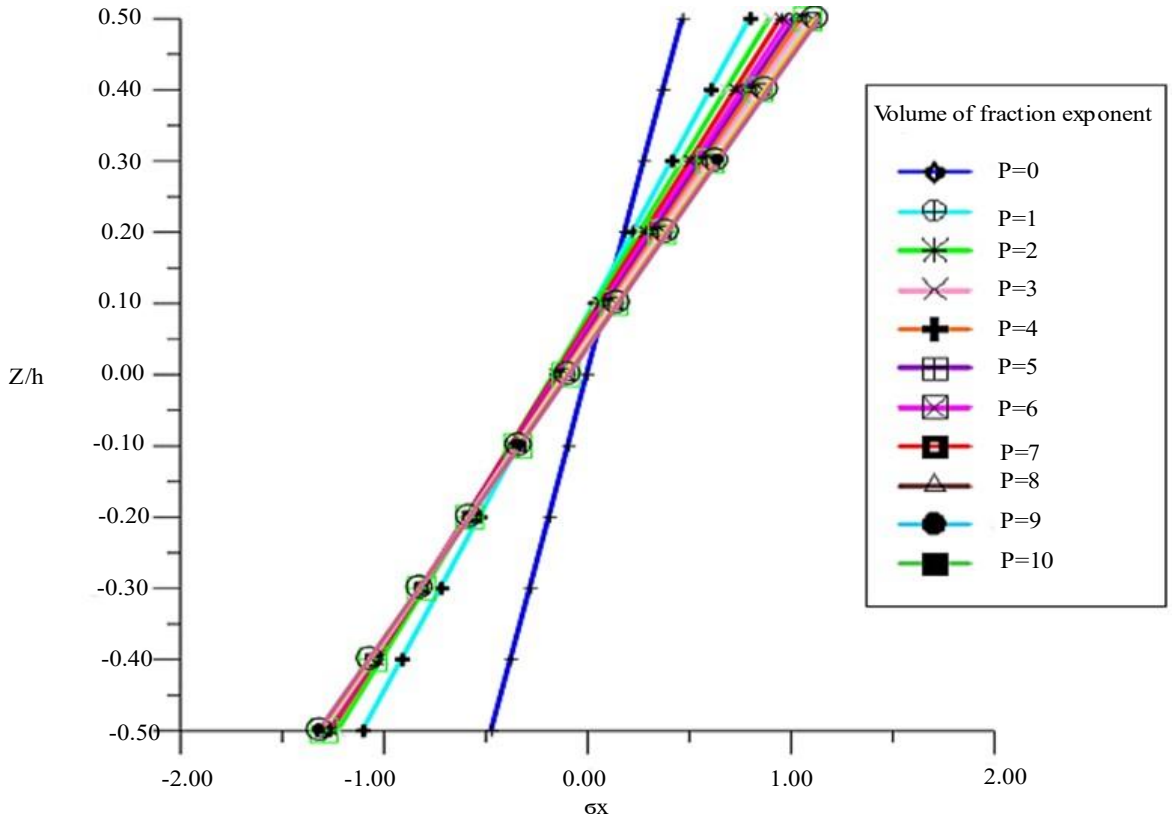

Figure 10. Dimensionless normal stress σ_x versus the thickness ratio of z/h functionally graded material (FGM) rectangular plate under linear loading.

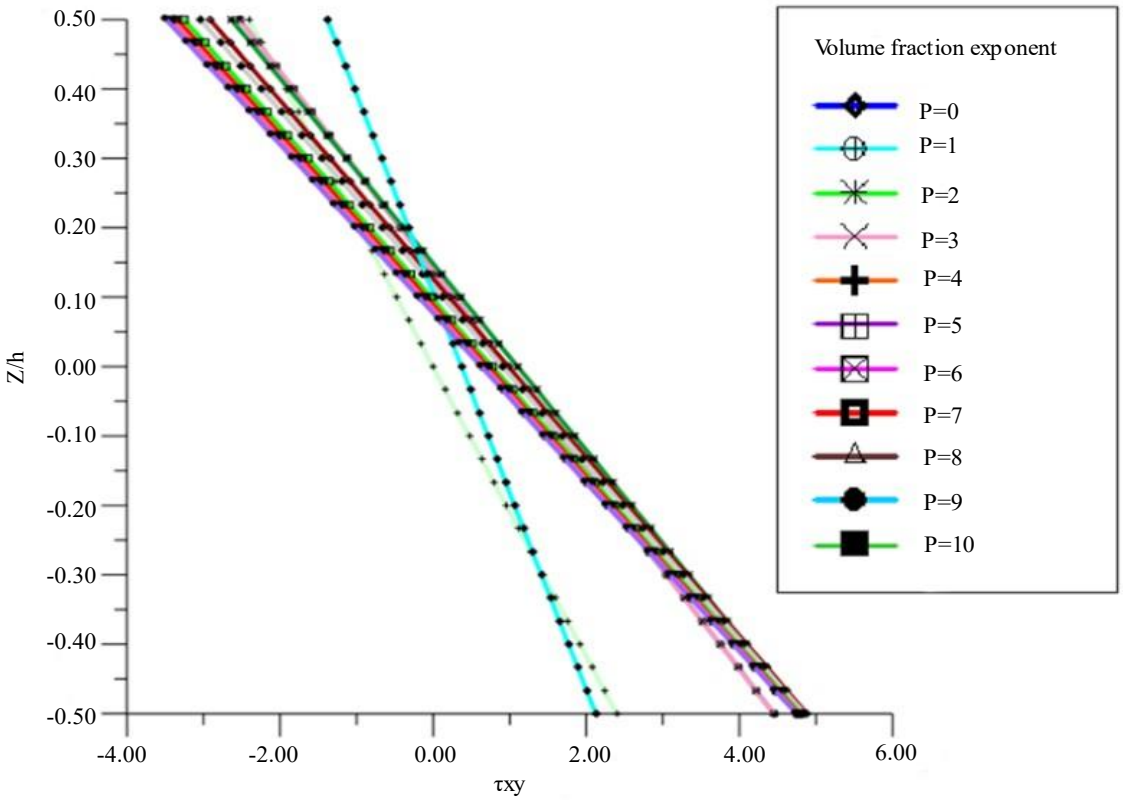

Figure 11. Dimensionless shear stress τ_{xy} versus thickness ratio of z/h functionally graded material (FGM) rectangular plate under linear loading.

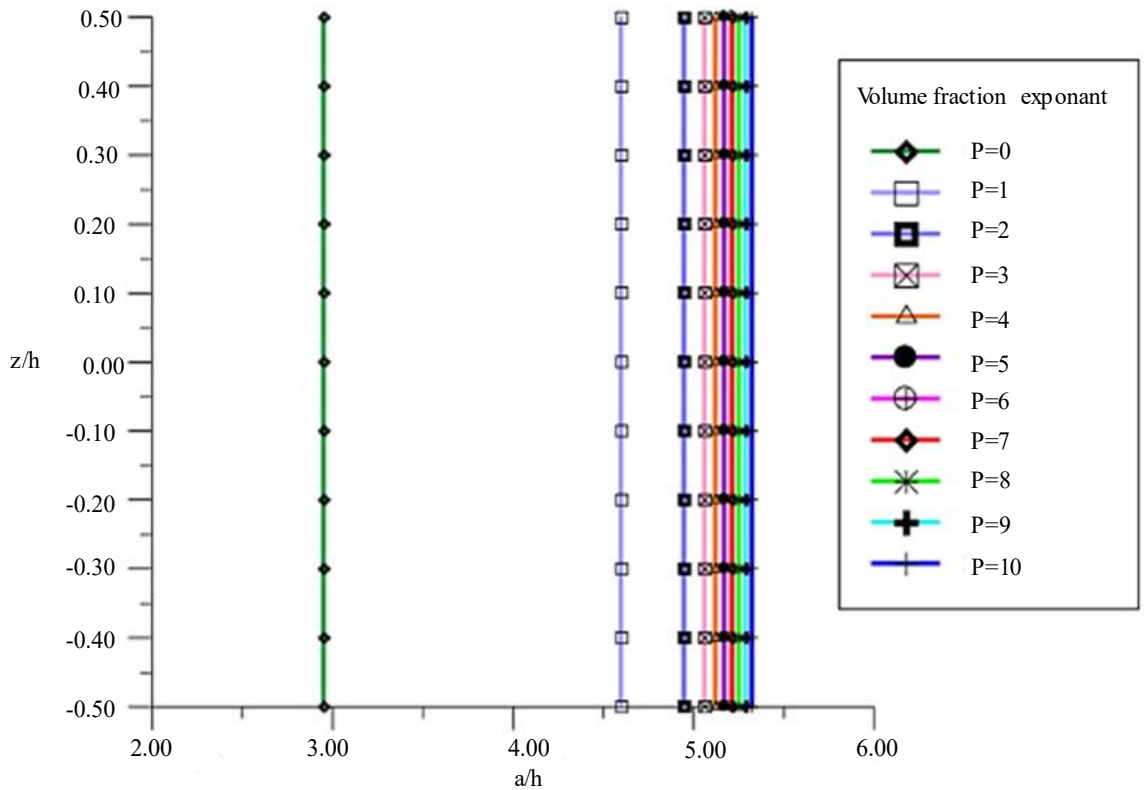

Figure 12. Dimensionless center deflection (w) for functionally graded material (FGM) rectangular plate under nonlinear stress as a function of side-to-thickness ratio (a/h) (5).

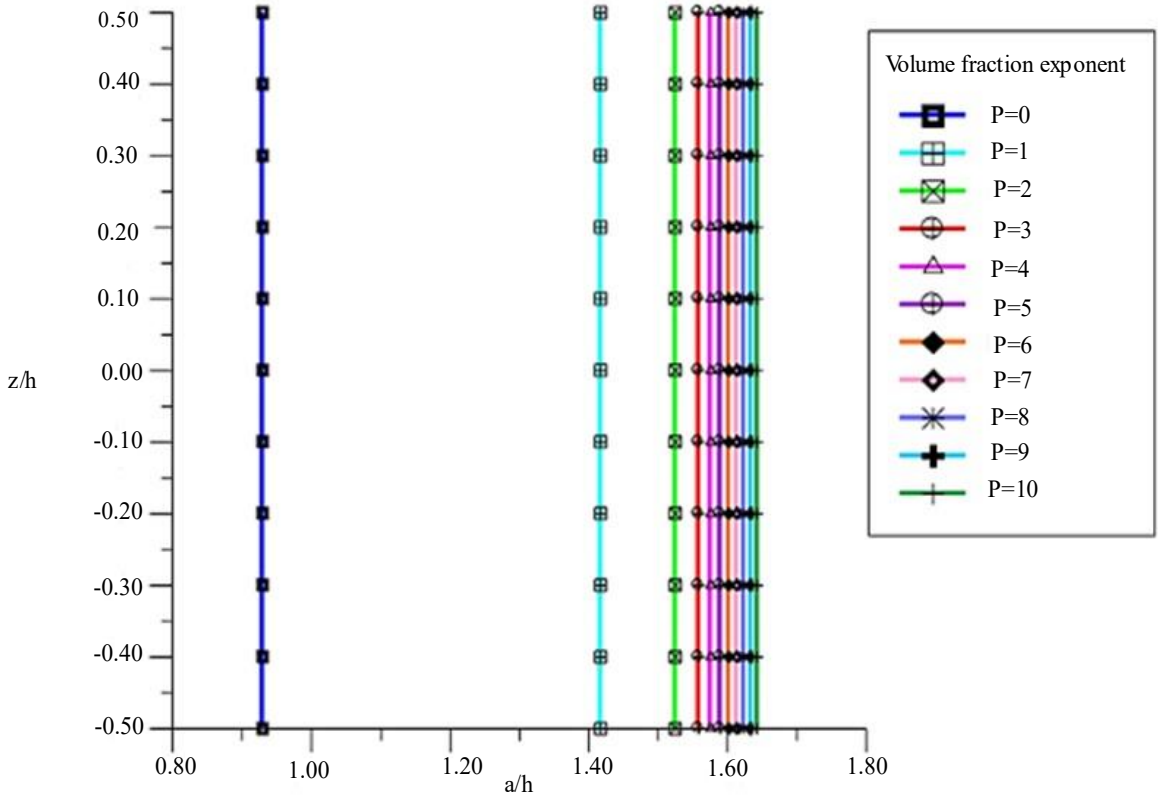

Figure 13. Dimensionless center deflection w versus side-to-thickness ratio a/h (10) for functionally graded material (FGM) rectangular plate under nonlinear loading.

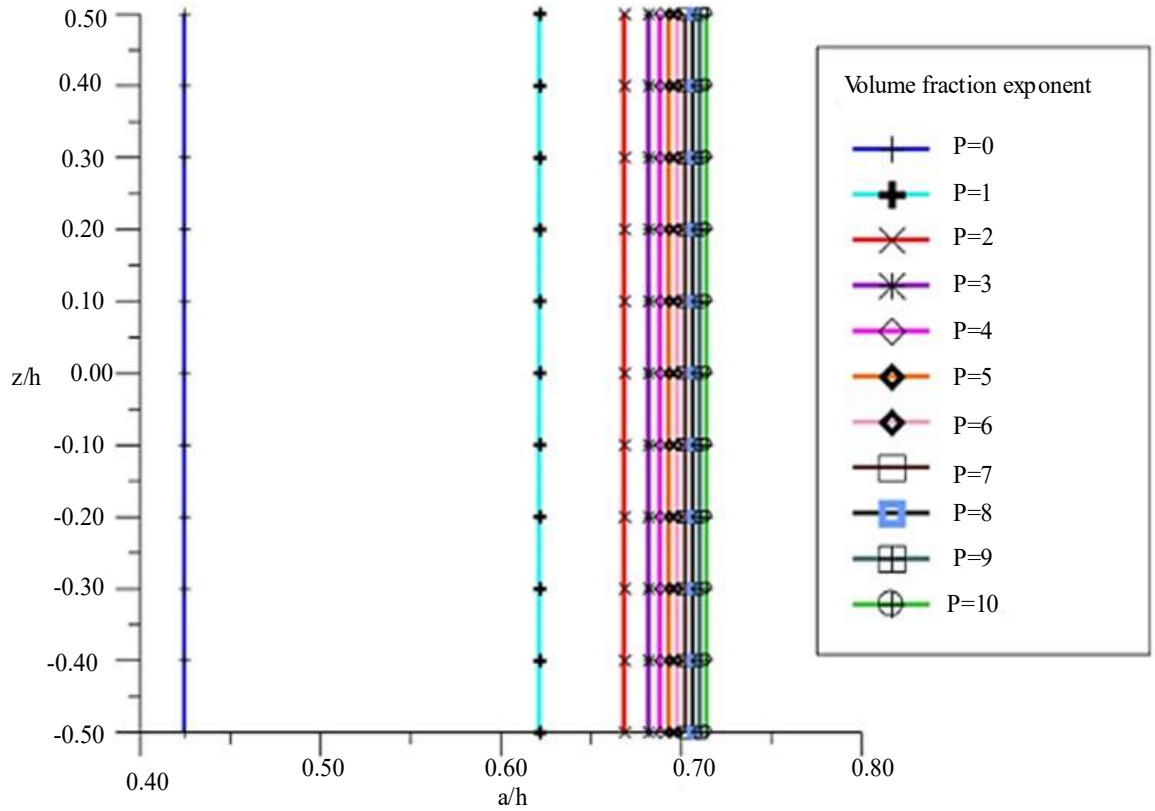

Figure 14. Dimensionless center deflection w versus side-to-thickness ratio a/h (20) for functionally graded material (FGM) rectangular plate under nonlinear loading.

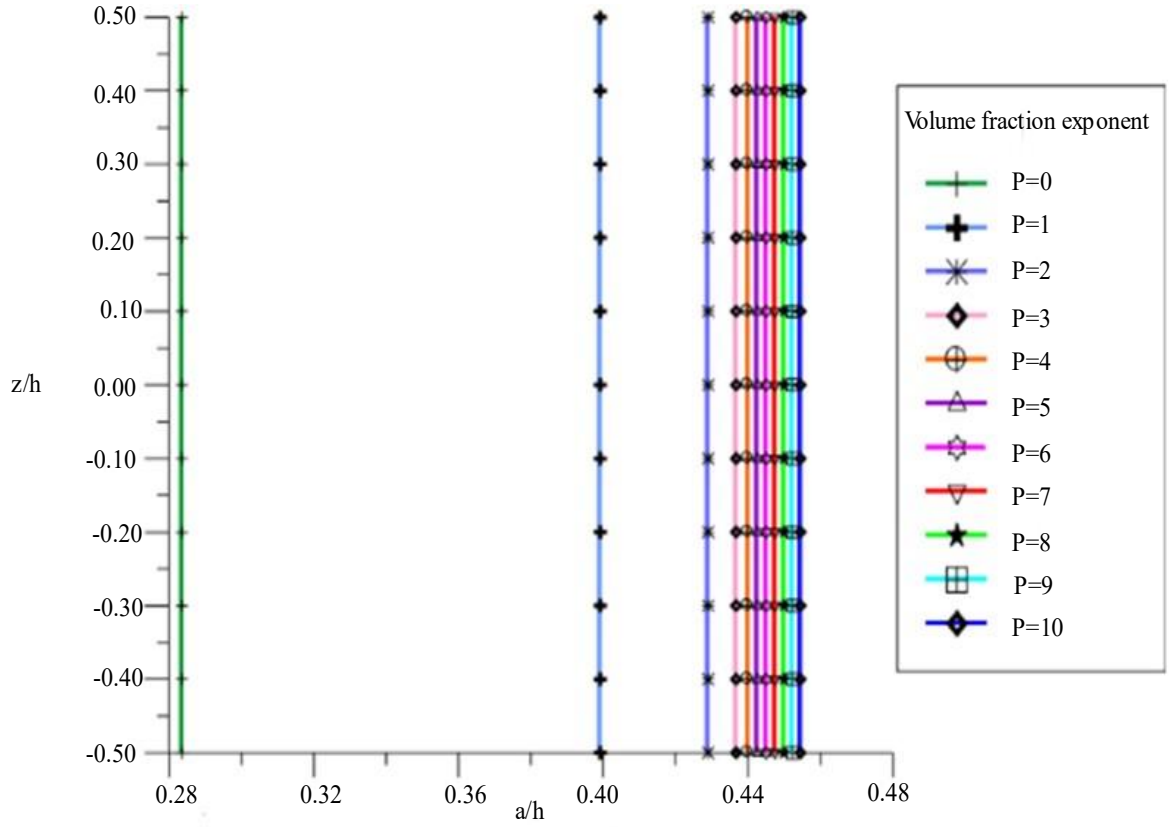

Figure 15. Dimensionless center deflection w for functionally graded material (FGM) rectangular plate under nonlinear force as a function of side-to-thickness ratio a/h (50).

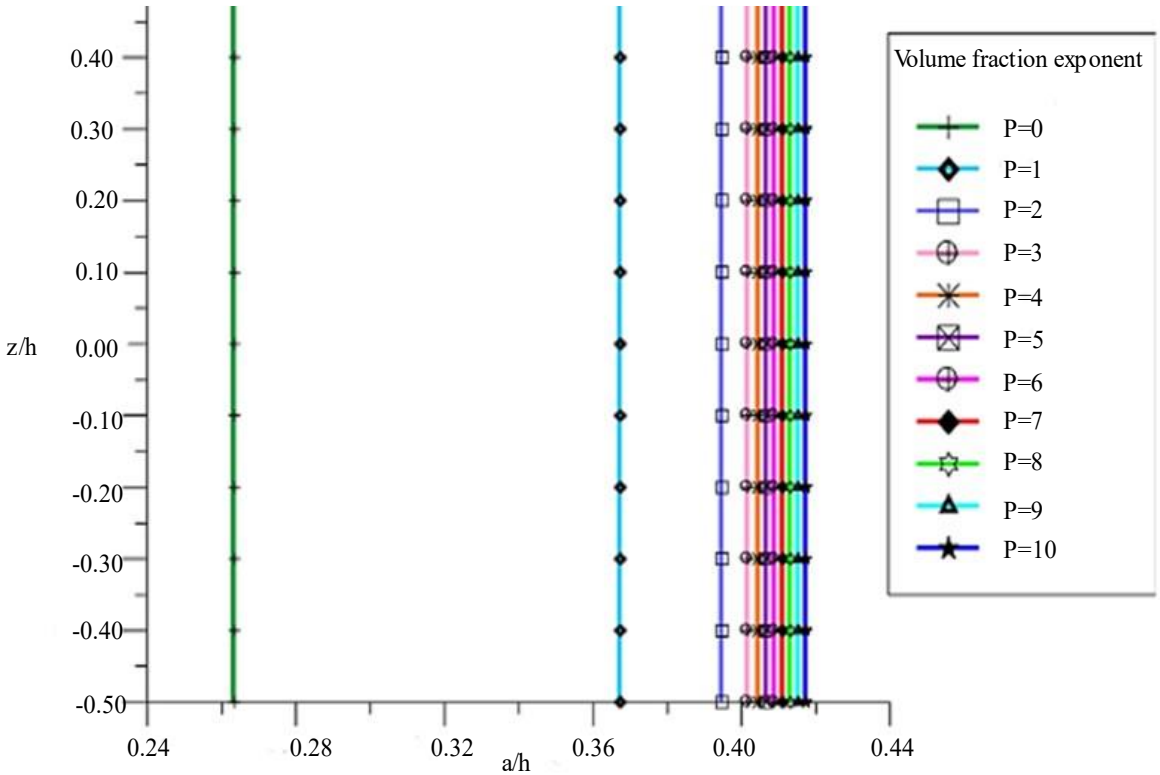

Figure 16. Dimensionless center deflection w for functionally graded material (FGM) rectangular plate under non-linear force versus side-to-thickness ratio a/h (100).

Table 4. Displacement model.

Model	Theory	Unknown Functions
CPT	Classical plate theory	3
FSDT	First-order shear deformation theory	5
TSDT	Third-order shear deformation theory	5
SSDT	Sinusoidal shear deformation theory	5
Present	Present refined plate theory	4
HSDT	Higher order shear deformation theory	4

Table 5. Effect of volume fraction exponent on the dimensionless and stresses of an functionally graded material (FGM) rectangular plate (a = 10h, b = 3a, q_0= 100, T = C = 0).

P	Theory	W	σ_K	r_{KF}
0	Present	0.8544	0.5113	0.7646
0	Zidi et al.	0.85891	0.51545	0.72797
0	TSDT	0.85891	0.51545	0.72797
0	SSDT	0.85887	0.51362	0.72784
0	FSDT	0.85892	0.51065	0.72949
0	CPT	0.83156	0.51065	0.72949
1	Present	1.1489	0.7503	1.4473
2	Present	1.2289	0.8085	1.5917
3	Present	1.2578	0.8228	1.6009
4	Present	1.2748	0.8273	1.5816
5	Present	1.2881	0.8299	1.5584
6	Present	1.2999	0.8320	1.5371
7	Present	1.3106	1.2948	1.5186
8	Present	1.3204	1.3020	1.5030
9	Present	1.3295	0.8387	1.4897
10	Present	1.3378	0.8409	1.4784

Table 6 illustrates the effects of the side-to-thickness ratio and elastic foundation parameters on the dimensionless deflection of FGM square plate under hygro-thermo-mechanical loads using the current four variables refined plate theory. Table 6 shows that when the a/h ratio increases, deflection decreases. This is because, in contrast to the plate's flexural behavior, temperature and moisture have a substantial effect on the plate's extensional behavior Table 7.

Table 6. Effect of volume fraction exponent and stresses of an functionally graded material (FGM) rectangular plate (a/h = 10, b = 3a, q_0= 100, t_0=t_2=0, t_1=10, c_0=c_2=0, c_1=100).

P	Theory	W	σ_K	r_{KF}
1	Present	1.8026	0.4697	1.5964
2	Zidi et al.	1.8071	0.4718	1.559
3	TSDT	1.8071	0.4718	1.559
4	SSDT	1.8070	0.4720	1.559
5	FSDT	1.8071	0.4690	1.5613
6	Present	2.6010	1.101	3.2845
7	Present	2.7862	1.2234	3.5898
8	Present	2.8598	1.2563	3.6111

P	Theory	W	σ_K	r_{KF}
9	Present	2.9060	1.2701	3.5736
10	Present	2.9425	1.2793	3.5276
11	Present	2.9740	1.2873	1.5371
12	Present	3.0020	1.2948	3.4474
13	Present	3.0273	1.3020	3.4157
14	Present	3.0499	1.3088	3.3885
15	Present	3.0694	1.3139	3.3653

Table 7. Impacts of a functionally graded material (FGM) square plate's dimensionless deflection and side-to-thickness ratio (a/h = 10, q_0=100, t_0=0, t_1=t_2=10, c_0=0, $c_1 = c_2$=100)

P	a/h = 5	a/h = 10	a/h = 20	a/h = 50	a/h = 100
0	2.9524	0.9296	0.4248	0.2836	0.2634
1	4.6013	1.4169	0.6217	0.3991	0.3673
2	4.9494	1.5247	0.6686	0.4289	0.3947
3	5.0626	1.5583	0.6821	0.4367	0.4016
4	5.1229	1.5755	0.6884	0.4400	0.4045
5	5.1726	1.5896	0.6935	0.4425	0.4067
6	5.2152	1.6018	0.6980	0.4450	0.4088
7	5.2543	1.6131	0.7024	0.4474	0.4110
8	5.2906	1.6237	0.7066	0.4498	0.4131
9	5.3242	1.6336	0.7106	0.4522	0.4152
10	5.3555	1.6429	0.7144	0.4544	0.4173

CONCLUSIONS

The following outcomes were obtained by using higher-order shear deformation theory to examine the hygrothermal analysis of functionally graded plates:

1. The displacement and stress results for the FGM plate produced by the current theory for both loading instances show great agreement with previous theories.
2. Theory avoids the need for a shear correction factor.
3. Compared to the five in the first-order shear deformation theory, the current theory has four governing equations and no unknown variables.
4. The results show that the higher-order shear deformation theories now in use include a lot of unknowns, and the current theory can be compared with them.

SCOPE OF THE WORK

Further research on the design of functionally graded plates for unique technical applications should make advantage of the formulation and technique that were developed.

- Plates with various other boundary and loading conditions can be analyzed.
- Elastic stability analysis of beams, plates, and shear stress can be carried out.
- Dynamic analysis of plates and shells can be carried out.
- Finite element analysis can be carried out based on this theory.
- This theory can be extended to nonlinear analysis of plates, beams, and shells.
- This theory can be extended to the analysis of composite plates and shells.

REFERENCES

1. Reddy JN. Analysis of functionally graded plates. Int J Numer Methods Eng. 2000; 47: 663–684.
2. Zhu P, Liew KM. A local kriging meshless method for free vibration analysis of functionally graded circular plates in thermal environments. Procedia Eng. 2012; 31: 1089–1094.

3. Alijani F, Amabili M. Non-linear dynamic instability of functionally graded plates in thermal environments. Int J Non-Linear Mech. 2013; 50, 109–126.
4. Ootao Y, Tanigawa Y. Three-dimensional solution for transient thermal stresses of the functionally graded rectangular plate due to non-uniform heat supply. Int J Mech Sci. 2005; 47: 1769–1788.
5. Chandel N, Manthena VR, Lamba NK. Thermoelastic behavior of a thin circular functionally graded material disk subjected to thermal loads. Int J Recent Innov Trends Comput Commun. 2015; 3 (2): 72–74.
6. Daouadji TH, Tounsi A, Bedia EAA. Analytical solution for bending analysis of functionally graded plates. Scientia Iranica. 2013; 20: 516–523.
7. Zenkour AM, Allam MNM, Radwan AF. Effects of transverse shear and normal strains on FG plates resting on elastic foundations under hygro-thermo-mechanical loading. Int J Appl Mech. 2014; 6: 1450063.
8. Daouadji TH, Tounsi A, Bedia EAA. A new higher order shear deformation model for static behavior of functionally graded plates. Adv Appl Math Mech. 2012; 5: 351–364.
9. Ghugal YM, Sayyad AS. Free vibration of thick orthotropic plates using trigonometric shear deformation theory. Latin Am J Solids Struct. 2011; 8: 229–243.
10. Mantari JL, Oktem KM, Soares CG. A new trigonometric shear deformation theory for isotropic, laminated composite and sandwich plates. Int J Solids Struct. 2012; 49: 43–53.
11. Thai HT, Kim SE. A simple higher-order shear deformation theory for bending and free vibration analysis of functionally graded plates. Composite Struct J. 2013; 96: 165–173.
12. Shimpi RP, Patel HG. Free vibrations of the plate using two variable refined plate theory. J Sound Vibr. 2006; 296: 979–999.
13. Mantari JL, Oktem AS, Soares CG. A new higher order shear deformation theory laminated composite and sandwich plates" Compos Part B Eng. 2012; 43 (3): 1489–1499.
14. Daouadji TH, Tounsi A, Bedia EAA. Theoretical analysis for static and dynamic behavior of functionally graded Plates. Mater Phys Mech. 2012; 14: 110–138.
15. Zenkour AM. Generalized shear deformation theory for bending analysis of FG plates. Appl Math Model. 2006; 30: 67–84.
16. Zidi M, Tounsi A, Houarib MSA, Bedia EAA, Beg OA. Bending analysis of FGM plates under hygro-thermo-mechanical loading using a four variable refined plate theory. Aerospace Sci Technol. 2014; 34: 24–34.

